Carbohydrate Polymers 98 (2013) 1203–1213

Contents lists available at ScienceDirect

Carbohydrate Polymers

journal homepage: www.elsevier.com/locate/carbpol

Analysis of xyloglucans by ambient chloride attachment ionization tandem mass spectrometry☆

Nelson R. Vinueza[a], Vanessa A. Gallardo[a], John F. Klimek[b], Nicholas C. Carpita[b], Hilkka I. Kenttämaa[a,*]

[a] Department of Chemistry, Purdue University, West Lafayette, IN 47907, USA
[b] Department of Botany and Plant Pathology, Purdue University, West Lafayette, IN 47907, USA

ARTICLE INFO

Article history:
Received 4 November 2012
Received in revised form 25 May 2013
Accepted 28 June 2013
Available online 8 July 2013

Keywords:
Xyloglucans
Electrospray ionization
Chloride attachment
Tandem mass spectrometry
Hymenaea courbaril, *Arabidopsis thaliana mur3*
Sequencing

ABSTRACT

Xyloglucan oligomers obtained upon enzyme digestion from *Hymenaea courbaril*, *Arabidopsis Columbia-0* and *mur3* were ionized and analyzed by using chloride anion attachment electrospray ionization (ESI) and tandem mass spectrometry. MW determination and structural elucidation of several xyloglucan oligomers was performed directly from the mixture solutions without sample pretreatment or derivatization. Sodium cation attachment was used to determine the number of xyloglucans present in the mixtures and their MWs. However, tandem mass spectrometry results showed that structure elucidation based on the sodium adducts is ambiguous. Chloride anion also forms stable adducts with these xyloglucans upon ESI. These adducts can be readily identified due to the chlorine isotope pattern. The mass spectral profile of xyloglucans obtained for the mixtures matches the HPAEC results, thus validating this methodology for the determination of the xyloglucan composition and the MW of each xyloglucan. Upon collisional activation in MS^2 experiments, the chloride anion adducts readily lose HCl, which helps verify the molecular weight of each xyloglucan. Isolating the resulting anion (deprotonated oligomer) and subjecting it to further collision-activated dissociation experiments (MS^n; $n = 3–4$) yields useful structural information that allows the differentiation between isomeric anions and hence determination of the sequence of the xyloglucan oligomers. The deprotonated oligomers fragment by a stepwise loss of sugar units from the reducing end.

1. Introduction

The plant primary cell wall is composed of cellulose microfibrils interlaced with cross-linking glycans and embedded in a gel matrix of pectic polysaccharides (Carpita & Gibeaut, 1993). The principal glycan that interlaces the cellulose microfibrils in dicot and nongraminaceous monocot plants is xyloglucan (XyG). XyG is characterized by a (1 → 4)-β-D-glucan backbone that, depending on species, has two to four consecutive glucose residues substituted by D-xylose in (1 → 6)-α-linkages, leaving one or more unbranched glucosyl residues (Sims, Munro, Currie, Craik, & Bacic, 1996; Tiné, Clovis, de Lima, Carpita, & Buckeridge, 2006). The xylose residue closest to the non-reducing end of the oligomer is never substituted further, but those nearer the reducing end may possess side-chain extensions of arabinopyranose, arabinofuranose, galactose, fucose, and other monosaccharides to give several kinds of oligomeric units that constitute a species-specific profile (Hoffman et al., 2005; Sims et al., 1996; Tiné et al., 2006). *Trichoderma viride* endo-β-glucanase, whose activity is restricted to unbranched residues, and similar enzymes cleave the glucan backbone to yield a species-specific profile of the oligomers.

In the genetic model plant, Arabidopsis, XyGs are composed of a fundamental heptamer, Xyl_3Glc_4, called XXXG in single-letter nomenclature (Fry, 1993). Five additional types of oligomers are formed by the addition of (1 → 2)-β-D-galactosyl (L) residues at the second and/or third xylose residue, to give XLXG, XXLG, and XLLG, and a subsequent addition of (1 → 2)-α-L-fucose (F) at the galactosyl unit attached to the first xylose from the reducing end, to give XXFG and XLFG (Table 1). Two non-allelic Arabidopsis mutant lines, *mur2* and *mur3*, were shown to have defects in the formation of XyG sidegroups. The *mur2* plants contain a missense mutation that causes a defect in the fucosyltransferase (AtFUT1; AT2G03220) that results in the absence of XyG fucosylation (Vanzin et al., 2002). The *mur3* plants have a defective galactosyl transferase (AtGalT; AT2G20370) that fails to add Gal to the xylosyl residue closest to

* Corresponding author at: Department of Chemistry, Purdue University, BRWN Building, 560 Oval Drive, West Lafayette, IN 47907, USA. Tel.: +1 765 494 0882; fax: +1 765 494 0239.
E-mail address: hilkka@purdue.edu (H.I. Kenttämaa).

0144-8617/$ – see front matter © 2013 The Authors. Published by Elsevier Ltd. All rights reserved.
http://dx.doi.org/10.1016/j.carbpol.2013.06.070

Table 1
Digested xyloglucan oligomers derived from *Arabidopsis thaliana* with their notations, MW and *m*/*z* values of ions formed upon chloride anion and sodium cation attachment.

Oligomer	Notation	MW (Da)	$[M+^{35}Cl]^-$	$[M+^{23}Na]^+$
Xyl Glc—Glc—Glc—Glc Xyl Xyl	XXXG	1062	1097	1085
Xyl Glc—Glc—Glc—Glc Xyl Xyl Gal	XLXG	1224	1259	1247
Gal Xyl Glc—Glc—Glc—Glc Xyl	XXLG	1224	1259	1247
Fuc Gal Xyl Glc—Glc—Glc—Glc Xyl	XXFG	1370	1405	1393
Gal Xyl Glc—Glc—Glc—Glc Xyl Gal	XLLG	1386	1421	1409
Fuc Gal Xyl Glc—Glc—Glc—Glc Xyl Gal	XLFG	1532	1567	1555

the reducing end (Madson et al., 2003). Without this Gal residue, fucosylation also fails to occur (Reiter, Chapple, & Somerville, 1997).

The above XyG oligomer profiles obtained for enzymatically degraded plant materials were determined by a combination of high performance anion-exchange chromatography (HPAEC) and electrospray ionization (ESI) mass spectrometry (Madson et al., 2003; Tiné et al., 2006; Vanzin et al., 2002). However, this approach has serious limitations. HPAEC resolves and allows quantification of the major oligomers, but the minor oligomers are not discernable. On the other hand, positive mode ESI-MS generates measurable sodium cation adducts for both the major and minor oligomers [XyG oligomer + Na^+] and has been used to identify and quantitate xyloglucan oligomers of different MW. Since the sodium cation adducts of XXLG and XLXG isomers have the same *m*/*z* value (1247), they have been differentiated based on the relative amounts of two fragment cations of *m*/*z* 659 and *m*/*z* 773, respectively, that are produced by cleavage in the middle of the glucan tetrasaccharide chain for each isomer (Madson et al., 2003). However, ESI-MS/MS data obtained for sodium cation adducts of xyloglucans is sometimes uninformative.

Tandem mass spectrometry in the negative ion mode has been demonstrated to yield unambiguous structural information for oligosaccharides (Pfenninger, Karas, Finke, & Stahl, 2002), making negative ion mode an attractive area of analysis of XyG. The combination of ESI with chloride anion dopant has proven to be an excellent method for the evaporation and ionization of underivatized oligosaccharides for several reasons (Cai & Cole, 2002; Cai, Jiang, & Cole, 2003; Jiang & Cole, 2005; Vinueza, Gallardo, Carpita, & Kenttämaa, 2012; Zhu & Cole, 2000; Zhu & Cole, 2001). Only a chloride anion adduct and no fragment ions are usually observed. The relative concentrations of the oligosaccharides can be determined based on the relative abundances of the adduct anions (Vinueza et al., 2012). The identification of chloride anion adducts is facilitated by the presence of chlorine isotopes. Further, the molecular weights of unknown oligosaccharides can be verified via observation of the loss of HCl upon CAD of the chloride anion adducts (MS/MS). We report here that formation of chloride anion adducts of XyG oligomers in negative mode ESI ionizes them efficiently and leads to no fragmentation. The stable chloride anion adducts can be subjected to collision-activated dissociation (CAD) to determine their structures. This method is a substantial improvement in the characterization of the sequences of complex unknown oligomers regardless of their origin.

2. Materials and methods

2.1. Plant lines and growth conditions

Seeds of Arabidopsis *Columbia-0* wild type and *mur3-1* mutant, originally obtained from Dr. Wolf-Dieter Reiter, University of Connecticut, have been propagated for several years at Purdue University. The seeds were suspended in water in Eppendorf tubes and chilled for three days at 4 °C to prime germination. Seeds were then sown in 4.5 in. pots with a soil mixture, supplemented with medium vermiculite and Osmocote, and the emerging plants were grown under greenhouse conditions at (25 ± 2 °C) and supplemental light to extend day length to 16 h. The pots were covered with a clear plastic top to raise humidity until plantlets had been established (about 7 d). Plants were watered as needed, approximately every 2–3 days. Leaves of the plants were harvested at 32 days. Seed storage xyloglucans of *Hymenaea courbaril* were provided by Dr. Marcos Buckeridge, University of São Paulo, Brasil.

2.2. Purification of XyGs

Leaves were frozen in liquid nitrogen and homogenized in a glass–glass grinder (Duall, Kontes Glass, Vineland, NJ) in 50 mM Tris[HCl], pH 7.2, supplemented with 1% (w/v) SDS (grinding buffer). Walls were collected by gentle centrifugation (1000 × *g*, 5 min), resuspended in grinding buffer, and incubated at 50 °C for 20 min before repeated centrifugation. Isolated walls were then washed three times in warm water (50 °C), warm 50% ethanol in water (v/v), and water at ambient temperature, with centrifugation after each washing step.

Pectic polysaccharides were extracted with 0.5% (w/v) ammonium oxalate, pH 7.0, in a 95 °C water bath for 1 h, followed by extraction with 0.1 M NaOH (supplemented with 3 mg ml^{-1} sodium borohydride to prevent end elimination) to remove other material and additional pectin. Walls were then extracted in 1.0 M NaOH (1 h), 4.0 M NaOH (1 h), and 4.0 M NaOH (15 h) at ambient temperature with constant stirring (all containing 3 mg ml^{-1} sodium borohydride). The 4 M NaOH extracts containing xyloglucans were passed through a glass-fiber filter (Whatman GF/C) to remove unsedimented wall remnants, and the eluent was chilled to ice temperature and acidified with glacial acetic acid until all the borohydride was destroyed. The fractions were dialyzed extensively against running deionized water for 36 h and then two consecutive portions of nanopure water for 4 h each before they were frozen in liquid nitrogen and freeze dried.

2.3. Determination of the distribution of the oligomers

About 1 mg of the freeze-dried preparations was dissolved in 0.5 ml of water by heating, and a small amount of insoluble material removed by centrifugation. 20 μl of a 1:100 dilution in 1 mM Na acetate, pH 5.5, of a suspension containing 0.1 U of (1 → 4)-endo-β-D-glucanase in 3.2 M ammonium sulfate (Megazyme, Ireland) were added, and the samples were incubated at 37 °C for 5 h or overnight. Samples were boiled for 2 min at the end of the incubation, and a

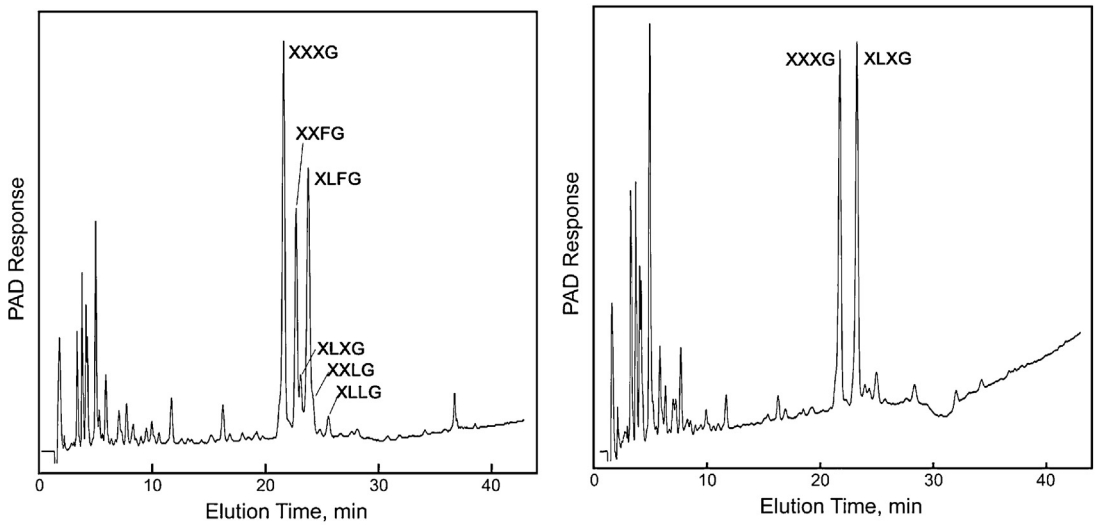

Fig. 1. (a) HPAEC profiles of Arabidopsis xyloglucan oligomers obtained upon enzymatic digestion from wild type (Columbia-0) and (b) *mur3-1*.

small amount of insoluble material removed by centrifugation. The clear supernatant solution was then directed to HPAEC or to MS.

2.4. High-performance anion-exchange chromatography

Digested samples were removed from 37 °C and boiled for 15 min. Samples were cooled to room temperature then centrifuged at 13,000 rpm for 5 min. Supernatant from each sample was transferred to a new Eppendorf tube. The *mur3* samples were diluted 1:30 with deionized water, mixed and centrifuged at 14,000 rpm for 5 min to remove a small amount of undissolved material. 100 μl were injected in a CarboPacPA-10 anion-exchange column (0.4 cm × 25 cm; Dionex) equilibrated in 0.2 M NaOH, and the oligomers were separated in a gradient of 0.2 M NaAc in 0.2 M NaOH at 0.35 ml min^{-1}.

2.5. Mass spectrometry

Mass spectrometry (MS) experiments were performed using a Thermo Scientific LTQ linear quadrupole ion trap (LQIT) mass spectrometer equipped with an electrospray ionization (ESI) source. All solutions were prepared at 10^{-3}–10^{-5} M concentrations in H_2O/CH_3OH (1:1, v/v). For ESI, 200 μl of 1 mM NH_4Cl in H_2O was added to 300 μl of 1 mM solution of the xyloglucan in sodium acetate. The solutions were infused into the mass spectrometer at a rate of 10 μl min^{-1} by using the integrated syringe drive of the LQIT and combined via a tee with 1:1(v/v) H_2O/CH_3OH solution delivered by a Finnigan Surveyor MS Pump Plus at a rate of 80 μl min^{-1}. The resulting mixture was infused into the ESI source to generate chloride adducts for the analytes. For the generation of sodium cation adducts, the same solutions discussed above were infused into the ESI source. Typical ESI conditions were: discharge current, 3.0 μA; sheath gas (N_2) flow, 45 (arbitrary units); auxiliary gas flow (N_2), 25 (arbitrary units); sweep gas flow (N_2), 1 (arbitrary units); and capillary temperature, 275 °C. Voltages for the ion optics were optimized for each analyte by using the tune feature of the LTQ Tune Plus interface. The experiments were performed using the advanced scan features of the LTQ Tune Plus interface. Collisionally activated dissociation (CAD) experiments involved isolation of the analyte by using a 2 *m*/*z* window (full width) and the application of an appropriate activation voltage (generally 10–25% of the "normalized collision energy" (NCE), as defined by the LTQ Tune Plus interface) for 30 ms. Xcalibur 2.0 software was used for both data acquisition and processing. All mass spectra shown are an average of at least 25 scans.

3. Results and discussion

3.1. Characterization of xyloglucan oligomers by HPAEC

The Arabidopsis *Columbia-0* wild-type showed a typical profile of primarily XXXG, XXFG, and XLFG after enzymatic digestion (Fig. 1a), whereas *mur3-1* gave primarily XXXG and XLXG (Fig. 1b), confirming that the genetic lesions result in an inactive xyloglucan-specific galactosyl transferase that decorates the Xyl residue closest to the reducing end of the oligomer (Madson et al., 2003). Confirmation of the presence and quantities of minor constituents required MS/MS analysis.

Seeds of the Brazilian tropical tree *H. courbaril* (jatobá) possess thickening cell walls rich in xyloglucans that are not fucosylated but are richly galactosylated (Buckeridge, 2010). Hymenaea

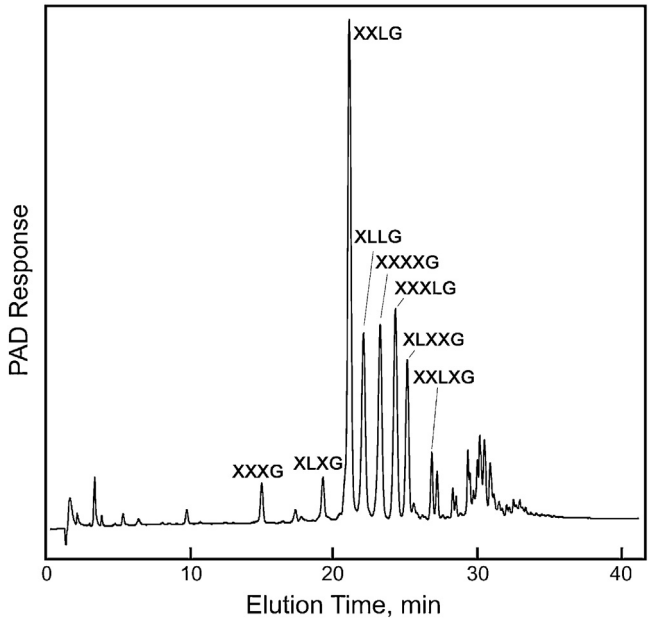

Fig. 2. HPAEC profile of seed storage xyloglucan oligomers from *Hymenaea courbaril*.

Table 2
Relative abundances of xyloglucan oligomers (M) based on $[M+^{35}Cl]^-$ and $[M+^{23}Na^+]$ ESI mass spectrometry and integration of the areas of peaks obtained by HPAEC.

Oligomer	HPAEC abundance	Relative abundance $[M+^{35}Cl]^-$	Relative abundance $[M+^{23}Na^+]$
Columbia-0			
XXXG	1.00	1.00	1.00
XXFG	0.57	0.39	0.34
XLFG	0.67	0.35	0.27
XLXG	0.07	~0.3[a]	~0.2[a]
XXLG	0.05	<0.1[a]	~0.1[a]
XLLG	0.05	0.10	0.11
mur3-1			
XXXG	0.99	0.97	1.00
XXFG	0.01	0.10	0.02
XLFG	0.04	0.08	0.03
XLXG	1.00	1.00	~0.7[a]
XXLG	0.02	Not detected	<0.1[a]
XLLG	0.01	0.15	0.03
Hymenaea courbaril			
XXXG	0.02	0.08	0.05
XXLG	1.00	1.00[a]	1.00[a]
XLXG	0.09	<0.1[a]	~0.2[a]
XLLG	0.41	0.33	0.29
XXXXG	0.42	0.25	0.18
XXXXG	0.27	|0.18|	|0.16|
XXLXG	0.08		
XXXLG	0.42		
XLLXG	Not determined	0.10	0.08

[a] Values for XLXG and XXLG were derived from diagnostic fragment anions observed upon CAD of the deprotonated XLXG and XXLG.

xyloglucans have an atypical structure containing XXXXG in addition to XXXG as the major fundamental units that are galactosylated (Tiné et al., 2006). In contrast to Arabidopsis XyGs, XXLG is the most abundant unit of the cellotetraose units, followed by XLLG, with only small amounts of XXXG and XLXG units. The XXXLG is the most abundant cellopentaose unit, with nearly equal amounts of XXXXG, followed by smaller amounts of XLXXG and of XXLXG (Fig. 2). Identification of additional, less abundant doubly and triply galactosylated oligomers could not be done and required MS/MS analysis.

3.2. Characterization of xyloglucan oligomers by MS

3.2.1. Arabidopsis Columbia-0

ESI with sodium cation attachment was first employed to detect XyG oligomers in *Arabidopsis Columbia-0* subjected to enzymatic digestion. Ions of *m/z* 1085 (XXXG), *m/z* 1247 (XLXG and XXLG), *m/z* 1393 (XXFG), *m/z* 1409 (XLLG) and *m/z* 1555 (XLFG) (Fig. 3a and Table 1) were detected, as expected. These ions were then isolated and subjected to CAD in order to examine their structures by MS^2. All sodium cation adducts were found to lose H_2O and also to undergo glycosidic bond cleavages and cross-ring cleavages (for XXXG, see Fig. 4a). Unfortunately, unambiguous structural information cannot be obtained from these fragmentations (for an example, see Fig. 4a). These results are a contrast with the CAD results obtained for the chloride anion adducts (for XXXG, see Fig. 4b), discussed in more detail below. ESI/chloride anion attachment of the oligomers derived from the *Arabidopsis Columbia-0* wild type gave anions of *m/z* 1097 (XXXG), *m/z* 1259 (XLXG and XXLG), *m/z* 1405 (XXFG), *m/z* 1421(XLLG) and *m/z* 1567 (XLFG), as expected (Fig. 3b and Table 2). Additional anions were also observed. These additional anions arise from impurities present in the XyG solution (see Section 2.3) that are easily ionized in negative ion mode but not in positive ion mode. None of these additional anions contain chlorine (based on lack of isotope peaks), which demonstrates that these anions are not oligosaccharides.

Table 3
Fragmentation of the chloride anion adducts of xyloglucans in MS/MS experiments and fragmentation of deprotonated xyloglucans in MS/MS/MS experiments.

Analysis	Mass (Da)	Interpretation
Common losses	−36	Loss of HCl
	−60	Loss of $C_2H_4O_2$ from a terminal glucose
	−78	Loss of $C_2H_4O_2 + H_2O$ from a terminal glucose
	−120	Loss of $C_4H_8O_4$ from a terminal glucose
	−162	Cleavage of a terminal glucose residue
	−294	Cleavage of xylose–glucose residue
	−312	Loss of $C_{11}H_{20}O_{10}$ from the glucose backbone
	−456	Cleavage of galactose–xylose–glucose residue

When the oligosaccharide ions corresponding to chloride anion adducts were isolated and subjected to CAD (in MS/MS experiments), they all lost HCl, which verifies that they were chloride anion adducts. For example, upon CAD, the chloride anion adduct of XXXG forms an anion of *m/z* 1061 that corresponds to deprotonated XXXG and is formed via HCl loss (Fig. 4b). Considering the relative abundances of the adduct ions formed in both negative (Cl^-) and positive (Na^+) ion mode revealed that XXXG is the most abundant oligomer, followed in order of abundance by XXFG, XLFG, XLXG, XXLG, and XLLG (Table 1). These results are in general agreement with the HPAEC profile for the enzyme digestion products obtained for *Arabidopsis Columbia-0* (Fig. 1a).

A final advantage of using chloride anion attachment ESI in mass spectrometric characterization of unknown oligosaccharides is that when the adducts' fragment ions formed upon HCl loss (upon CAD in MS/MS experiments) are isolated and subjected to further CAD (MS/MS/MS), valuable structural information is obtained for the oligosaccharides even in cases where MS/MS does not yield adequate structural information. The major fragmentation pathways observed in MS/MS/MS experiments for deprotonated XyG oligomers are shown in Scheme 1 and in Table 3. For example, deprotonated XXXG forms a fragment anion of *m/z* 899 upon CAD, which indicates the loss of the terminal glucose unit via cleavage of a glycosidic bond. The ion of *m/z* 899 represents the deprotonated fragment XXX (which was verified by high-resolution measurements), which consists of three glucose units bound by (1 → 4) linkages as the backbone, each of which has a xylose unit bonded to it by a (1 → 6)-linkage. The anion of *m/z* 899 fragments to yield an anion of *m/z* 605, which represents deprotonated XX. Hence, the deprotonated oligomer XXXG fragments by a stepwise loss of mono- and/or disaccharide units from the reducing end. The same was found to occur for the other XyG oligomers (Table 4).

CAD of the chloride anion adducts of the mixture of isomers XLXG and XXLG (*m/z* 1259, Scheme 2), which cannot be studied separately as they have exactly the same mass, generates several fragment anions, including those of *m/z* 1223, 1163, 1145, 1061, 983, 767 and 605. The anion of *m/z* 1223 corresponds to the deprotonated molecule formed via HCl loss (Scheme 2). The other fragment anions arise from decomposition of the ion of *m/z* 1223. For example, the anion of *m/z* 1163 is generated by cross-ring cleavage in the terminal glucose unit resulting in the loss of a molecule of MW of 60 Da ($C_2H_4O_2$), and the anion of *m/z* 1145 is generated by the loss of the same molecule followed by dehydration ($-C_2H_4O_2-H_2O$). The anion of *m/z* 1061 is formed by the cleavage of the glycosidic bond to the terminal glucose (resulting in the loss of a glucose molecule with MW of 162 Da) in the deprotonated isomeric oligomers (*m/z* 1223). The anion of *m/z* 983 is formed by a cross-ring cleavage followed by dehydration ($-C_2H_4O_2-H_2O$) of the anion of *m/z* 1061.

The last two fragment anions listed above, those of *m/z* 767 and *m/z* 605 (Fig. 5c), demonstrate the presence of both isomers XLXG and XXLG in the mixture since only the chloride anion adduct of XXLG can fragment to give the anion of *m/z* 605 (deprotonated XX)

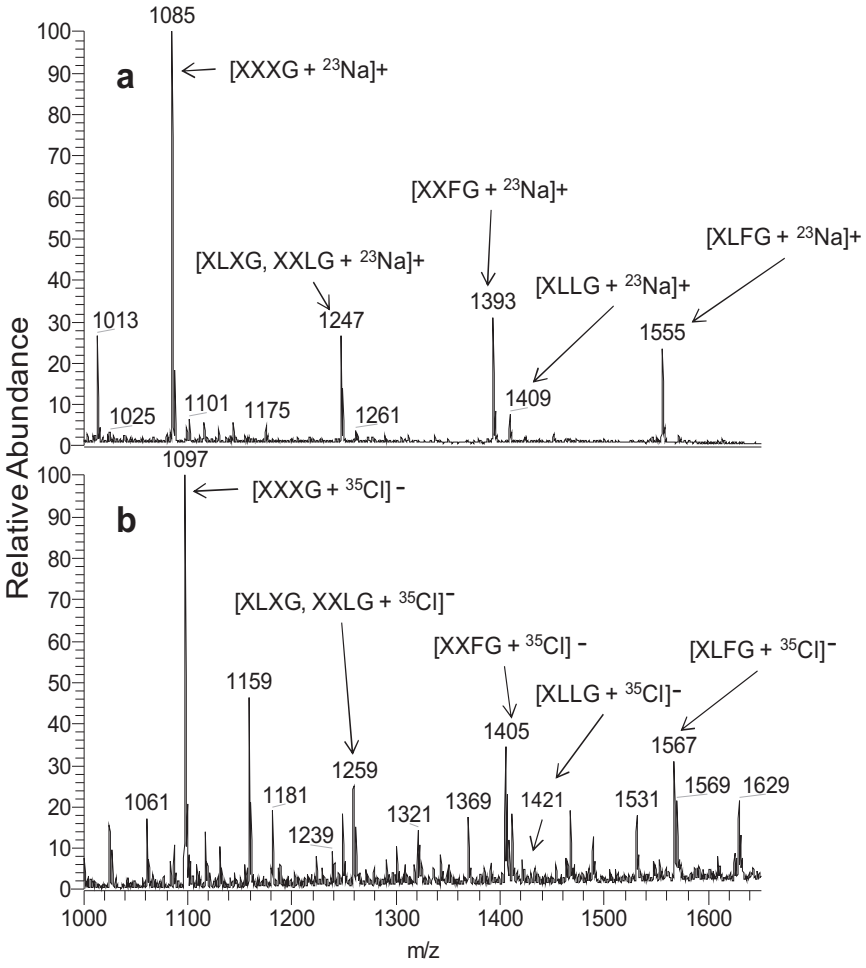

Fig. 3. Mass spectra obtained for XyG oligomers derived from Columbia-0 measured by using (a) ESI/Na^+ addition and (b) ESI/Cl^- addition.

while the chloride anion adduct of XLXG gives a fragment anion of *m*/*z* 767 (deprotonated XL; Fig. 5b). Since formation of both anions involves a glycosidic bond cleavage to eliminate a disaccharide (LG or XG), their reaction rates are likely to be similar. The approximate ratio of the abundances of the anions *m*/*z* 767 and 605 is 3:1, which suggests that the XLXG oligomer is more abundant than XXLG in the mixture.

In agreement with the fragmentation behavior described above, CAD of the chloride anion adduct of XXFG (*m*/*z* 1405, Supplemental information, Table 1) generates fragment anions of *m*/*z* 1369, 1039, 1291, and 1207 (among others), which arise via pathways analogous to those discussed above. The anion of *m*/*z* 1369 is generated via HCl loss from the chloride anion adduct of XXFG. The other fragments anions arise from decomposition of this deprotonated molecule (*m*/*z* 1369). These results were confirmed by performing isolation and CAD of the anion of *m*/*z* 1369 (MS^3). The anion of *m*/*z* 1369 fragments to form the anion of *m*/*z* 1309 via loss of $C_2H_4O_2$. The fragment anion of *m*/*z* 1291 is generated by loss of $C_2H_4O_2$ and loss of H_2O from the anion of *m*/*z* 1369 while loss of the terminal glucose yields the fragment anion of *m*/*z* 1207 (deprotonated XXF). Deprotonated XXF fragments further to give an anion of *m*/*z* 601 (deprotonated F; Scheme 3) via the loss of neutral XX (606 Da). The anion of *m*/*z* 601 represents a deprotonated oligomer that contains glucose, xylose, galactose and fucose.

3.2.2. *mur3-1*

The analysis of degraded Arabidopsis mutant *mur3-1* by ESI chloride anion attachment MS showed two main chloride anion

Table 4
Key fragment anions used for the sequencing of deprotonated xyloglucan oligomers in MS/MS/MS experiments.

Xyloglucan	XX *m*/*z* 605	XL *m*/*z* 767	XXX *m*/*z* 899	XXL/XLX *m*/*z* 1061	XLL *m*/*z* 1223
XXXG	Y		Y		
XXLG	Y			Y	
XLXG		Y		Y	
XXFG	No key anions				
XLFG		Y			
XXXXG	Y		Y		
XLLG		Y		Y	Y
XLXXG		Y		Y	
XXLXG	Y				
XXXLG	Y		Y		
XLLXG		Y			Y

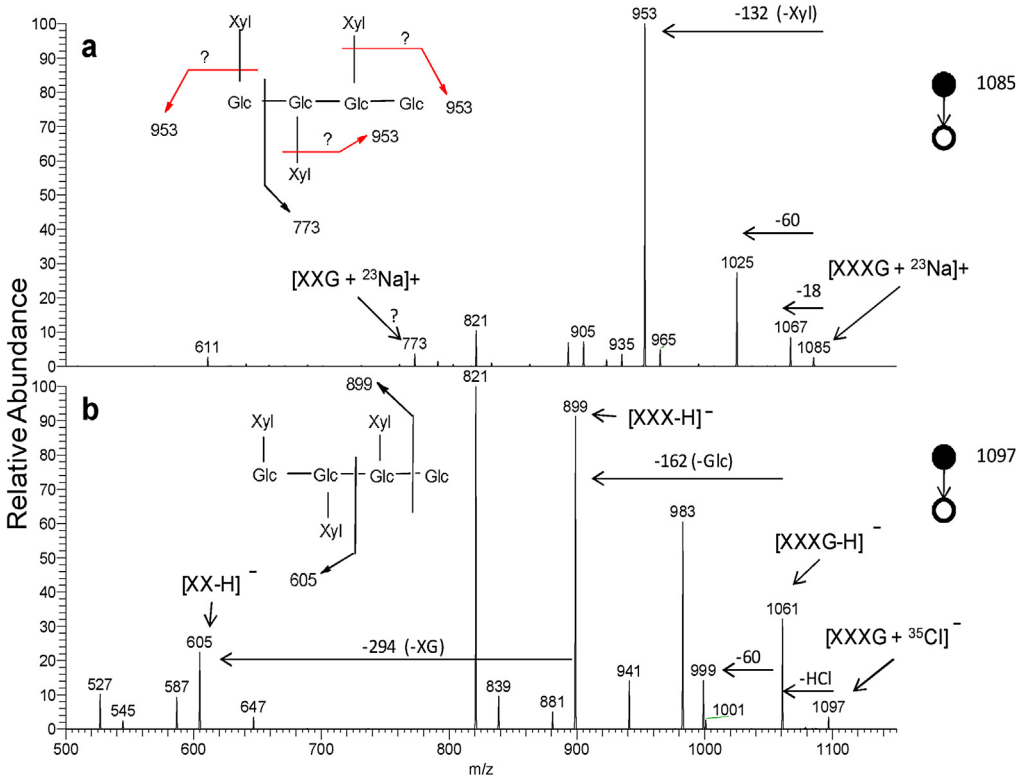

Fig. 4. (a) MS^2 spectrum obtained after CAD of the sodium adduct of XXXG (*m*/*z* 1085) derived from Columbia-0. The loss of a neutral molecule with MW of 18 Da (H_2O) yields a cation of *m*/*z* 1067, a sodium adduct of dehydrated XXXG. Loss of a xylose molecule with MW of 132 Da via the cleavage of a glycosidic bond yields a fragment cation of *m*/*z* 953. The structure of this cation cannot be readily deduced since there are three xylose units that can be lost. (b) MS^2 spectrum obtained after CAD of the chloride anion adduct of XXXG (*m*/*z* 1097) derived from Columbia-0. The loss of a neutral molecule with MW of 36 Da (HCl) yields an anion of *m*/*z* 1061, deprotonated XXXG. Loss of a glucose molecule with MW of 162 Da from deprotonated XXXG (*m*/*z* 1061) via cleavage of the terminal glucose residue yields a fragment anion of *m*/*z* 899, deprotonated XXX. Loss of a glucose–xylose residue with MW of 294 Da via the cleavage of a glucose–xylose residue from deprotonated XXX yields a fragment anion of *m*/*z* 605, deprotonated XX. These reactions reveal the sequence of XXXG.

adducts, the anions of *m*/*z* 1097 and 1259 (Fig. 5a). These adducts have the same abundance, which is in general agreement with the HPAEC results (Fig. 1b and Table 2). The anion of *m*/*z* 1097 corresponds to the chloride anion adduct of XXXG based on the finding that upon CAD, it yields the fragment anion of *m*/*z* 605 (deprotonated XX) and of *m*/*z* 899 (deprotonated XXX) (Fig. 6). On the other hand, the anion of *m*/*z* 1259 (likely deprotonated XLXG) gives the fragment anions of *m*/*z* 1223, 1145, 1061, 983, and 767 upon CAD.

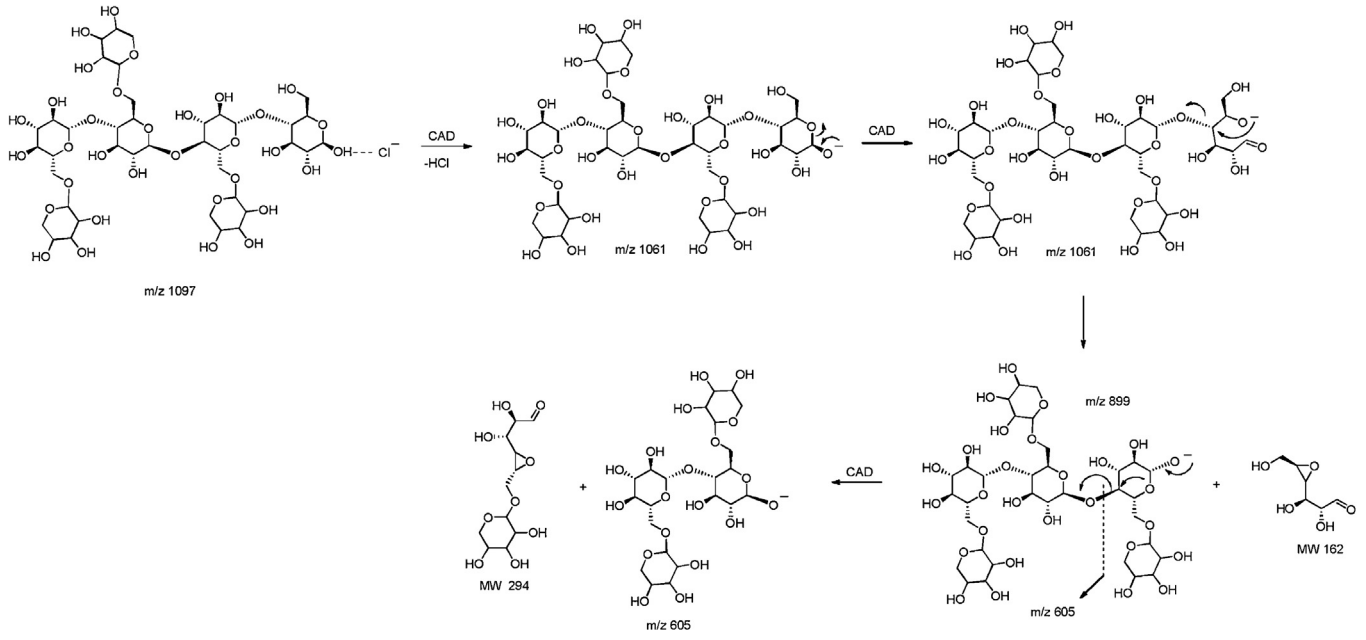

Scheme 1.

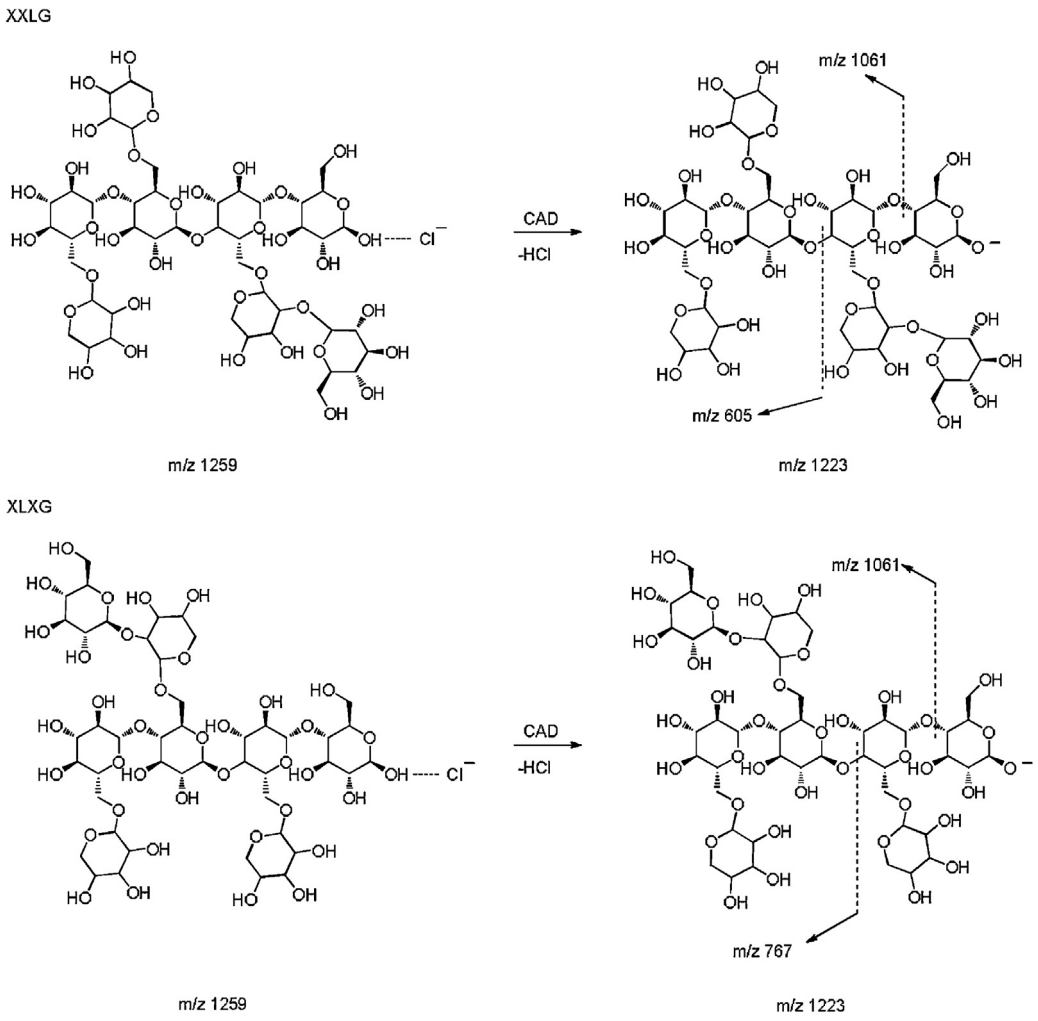

Scheme 2.

An anion of *m*/*z* 605 (corresponding to deprotonated XX) that was detected for the chloride anion adduct of *m*/*z* of 1259 corresponding to a mixture of deprotonated XLXG and XXLG (derived from *Columbia-0*) was not observed. Hence, the anion of *m*/*z* 1259 derived from *mur3-1* is the chloride anion adduct of XLXG and not XXLG. This was confirmed by the observation of the fragment anion of *m*/*z* 767 (deprotonated XL) characteristic of XLXG (Fig. 7). The finding that the primary galactosylated XyG oligomer of *mur3-1* is XLXG is in agreement with the HPAEC results (Table 2). Further analysis by CAD of the fragment anion of *m*/*z* 767 (deprotonated XL) shows the generation of a fragment anion of *m*/*z* 455 (deprotonated L) via the loss of galactose and xylose (Fig. 6), as expected.

3.2.3. *H. courbaril*

As expected based on HPAEC results, chloride anion attachment ESI/MS of degraded *Hymenaea* gave anions of *m*/*z* 1097 (XXXG), *m*/*z* 1259 (XLXG and XXLG), *m*/*z* 1391 (XXXXG), *m*/*z* 1421 (XLLG), *m*/*z* 1553 (XLXXG, XXLXG and XXXLG) and *m*/*z* 1715 (XLLXG, XLXLG and XXLLG), in addition to anions not corresponding to xyloglucans since they were not chloride anion adducts (Fig. 8; Supplemental information, Table 2). Upon CAD, the chloride anion adducts of the mixture of XLXG and XXLG (*m*/*z* 1259) generate the fragment anions of *m*/*z* 1223, 1163, 1145, 1061, 983, 767, 605 and 455, among others (Supplemental information, Table 2). These fragment anions were also observed for the chloride anion adducts of the mixture of XLXG and XXLG (*m*/*z* 1259) derived from *Columbia-0*. Interestingly, the ratio of the fragment anions of *m*/*z* 767 and 605 was drastically different from that observed for *Columbia-0*, the fragment anion of *m*/*z* 605 being more abundant for the *Hymenaea* sample (Supplemental information, Figure 1). These results reveal an excess of XXLG compared to XLXG, which was also observed by Tiné et al. (2006).

CAD of the chloride anion adduct of XXXXG (*m*/*z* 1391) generated fragment anions of *m*/*z* 1355, 1277, 1235, 1193, 1115, 899, 821 and 605, among others (Supplemental information, Figure 2). The anions of *m*/*z* 1193, 899 and 605 are the most important ones for sequencing of XXXXG (Figure 9). Upon CAD, the loss of a glucose residue (162 Da) from the deprotonated XXXXG (*m*/*z* 1355) produces the fragment anion of *m*/*z* 1193 (deprotonated XXXX). CAD of the anion of *m*/*z* 1193 generates two key fragment anions, those of *m*/*z* 899 and 605. These anions correspond to deprotonated XXX and deprotonated XX, respectively.

CAD of the chloride anion adduct of XLLG (*m*/*z* 1421; Supplemental information, Table 2) generated fragment anions of *m*/*z* 1385, 1325, 1307, 1223, 1145, 767 and 455, among others. The fragment anions of *m*/*z* 1385, 1325 and 1307 correspond to loss of HCl, $C_2H_4O_2$ or $C_2H_4O_2 + H_2O$, respectively, from the chloride anion adduct of XLLG (*m*/*z* 1421). The fragment anion of *m*/*z* 1223 (deprotonated XLL) corresponds to the loss of a glucose residue from deprotonated XLLG After isolation and CAD, this anion generates a key fragment ion of *m*/*z* 767, which corresponds to deprotonated XL and is formed via the loss of a molecule with MW of 456 Da (L).

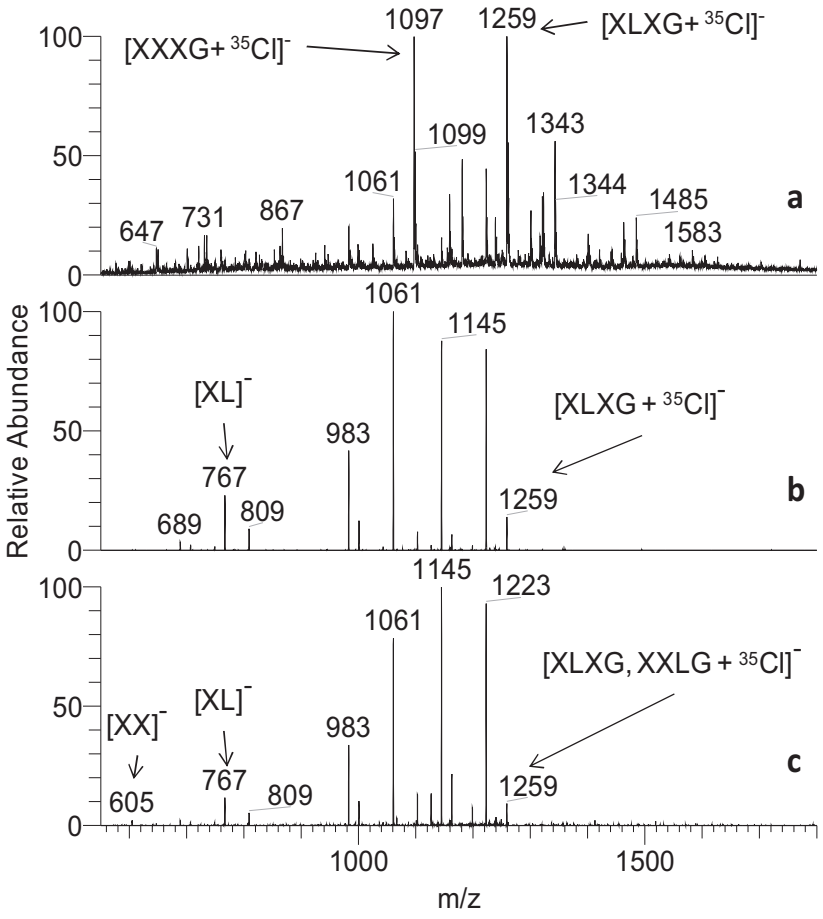

Fig. 5. (a) Mass spectra obtained for enzymatically digested *mur3-1* by chloride anion attachment ESI/MS. (b) MS^2 spectrum obtained after CAD of the chloride anion adduct of XLXG (*m*/*z* 1259) from *mur3-1*. (c) MS^2 spectrum obtained after CAD of the chloride anion adducts of XLXG and XXLG (*m*/*z* 1259) from Columbia-0.

Hence, the presence of a galactose residue at the second xylose unit was verified (Supplemental information, Figure 3).

CAD of the chloride anion adducts of a mixture of XLXXG, XXLXG and XXXLG (*m*/*z* 1553; Supplemental information, Table 2) generated the fragment anions of *m*/*z* 1517, 1457, 1439, 1397, 1355, 1295, 1227, 1103, 1061, 983 and 455. Other fragment anions, those of *m*/*z* 899, 767 and 605, were also observed although in a very low abundance. The most informative fragment anions are those of *m*/*z* 1355, 1061, 899, 767 and 605. The anion of *m*/*z* 1355 arises from the loss of a glucose residue from the three deprotonated isomeric XyGs formed upon HCl loss from their chloride anion adducts, and thus corresponds to three isomeric deprotonated oligomers, XLXX, XXLX and XXXL. These anions were subjected to CAD (MS^3) and the fragment anions of *m*/*z* 1061, 899, 767 and 605 were generated. The fragment anion of *m*/*z* 1061 is formed via the loss of a molecule of MW 294 Da (X) to yield two isomeric deprotonated oligomers XLX and XXL. The fragment anions of *m*/*z* 767 and 605 correspond to deprotonated XL and XX, respectively, as discussed above. The fragment ion of *m*/*z* 899 corresponds to deprotonated XXX, which was also observed when the chloride anion adduct of XXXXG was

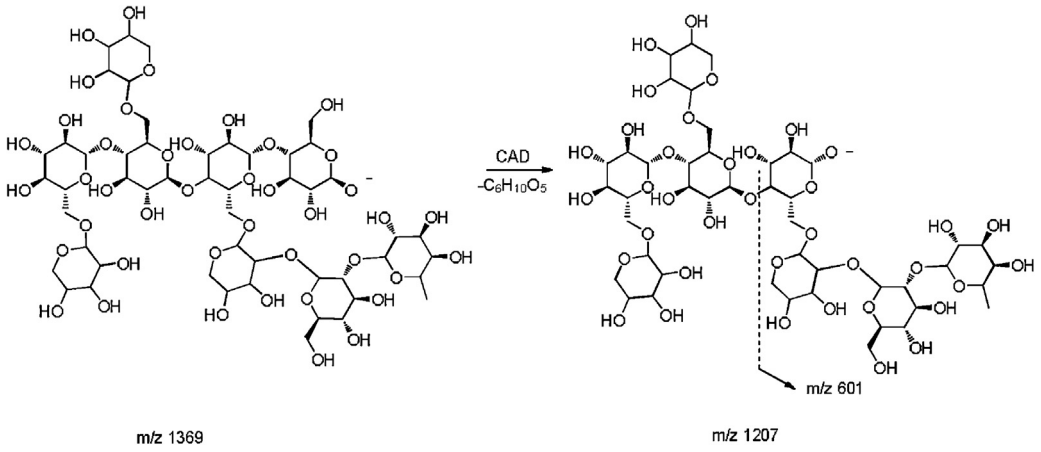

Scheme 3.

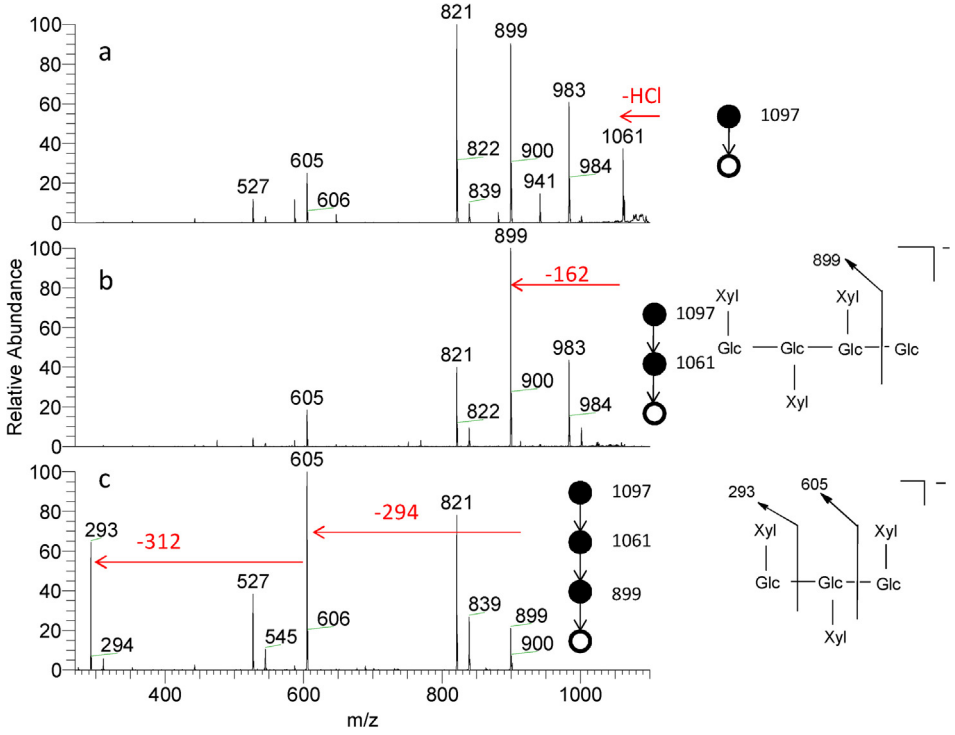

Fig. 6. (a) MS^2 spectrum obtained after CAD of the chloride anion adduct of XXXG (*m*/*z* 1097) derived from *mur3-1*. The loss of a neutral molecule with MW of 36 Da (HCl) yields an anion of *m*/*z* 1061, deprotonated XXXG. (b) MS^3 spectrum obtained after CAD of deprotonated XXXG (*m*/*z* 1061). Loss of a molecule with MW of 162 Da via the cleavage of a terminal glucose residue yields a fragment ion of *m*/*z* 899, deprotonated XXX. (c) MS^3 spectrum obtained after CAD of deprotonated XXX (*m*/*z* 899). Loss of a molecule with MW of 294 Da via the cleavage of a glucose–xylose residue from deprotonated XXX yields a fragment anion of *m*/*z* 605, deprotonated XX.

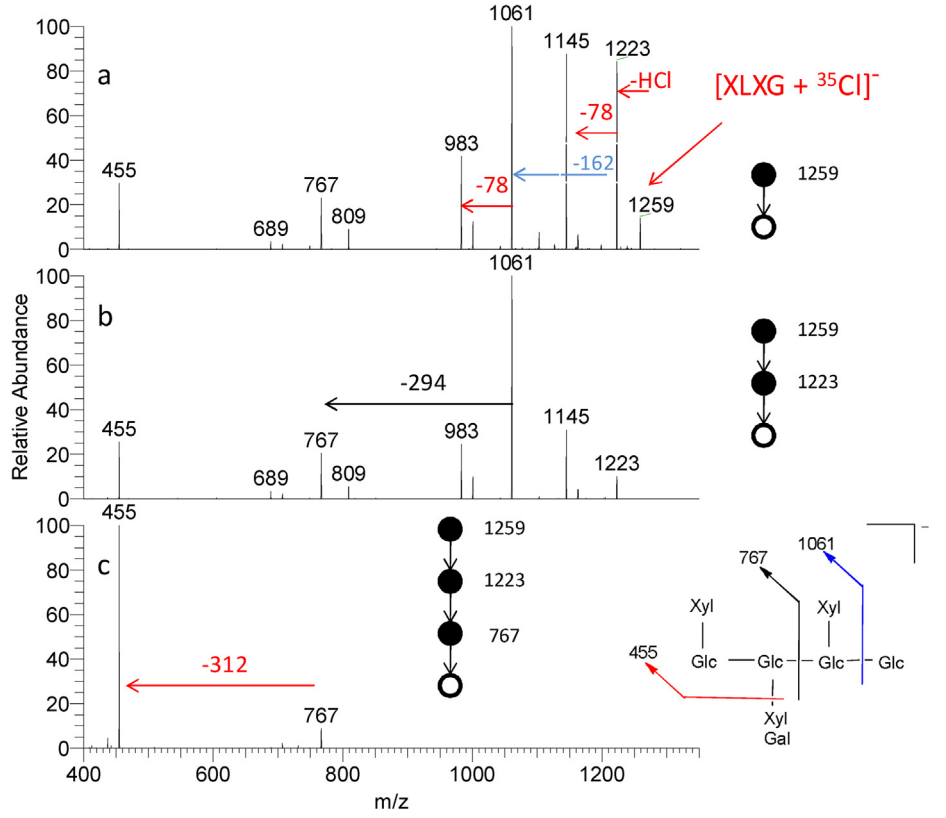

Fig. 7. (a) MS^2 spectrum obtained after CAD of the chloride anion adduct of XLXG (*m*/*z* 1259) derived from *mur3-1*. The loss of a neutral molecule with MW of 36 Da (HCl) yields an anion of *m*/*z* 1223, deprotonated XLXG. (b) MS^3 spectrum obtained after CAD of deprotonated XLXG (*m*/*z* 1223) reveals the loss of a molecule with MW of 162 Da via the cleavage of a terminal glucose residue to yield a fragment ion of *m*/*z* 1061, deprotonated XLX. Loss of a neutral molecule with MW of 294 Da via the cleavage of a glucose–xylose residue from deprotonated XLX yields a fragment anion of *m*/*z* 767, deprotonated XL (c) MS^3 spectrum obtained after CAD of deprotonated XL (*m*/*z* 767) reveals the loss of a molecule with MW of 312 Da via the cleavage of $C_{11}H_{20}O_{10}$ from the glucose backbone to yield a fragment anion of *m*/*z* 455.

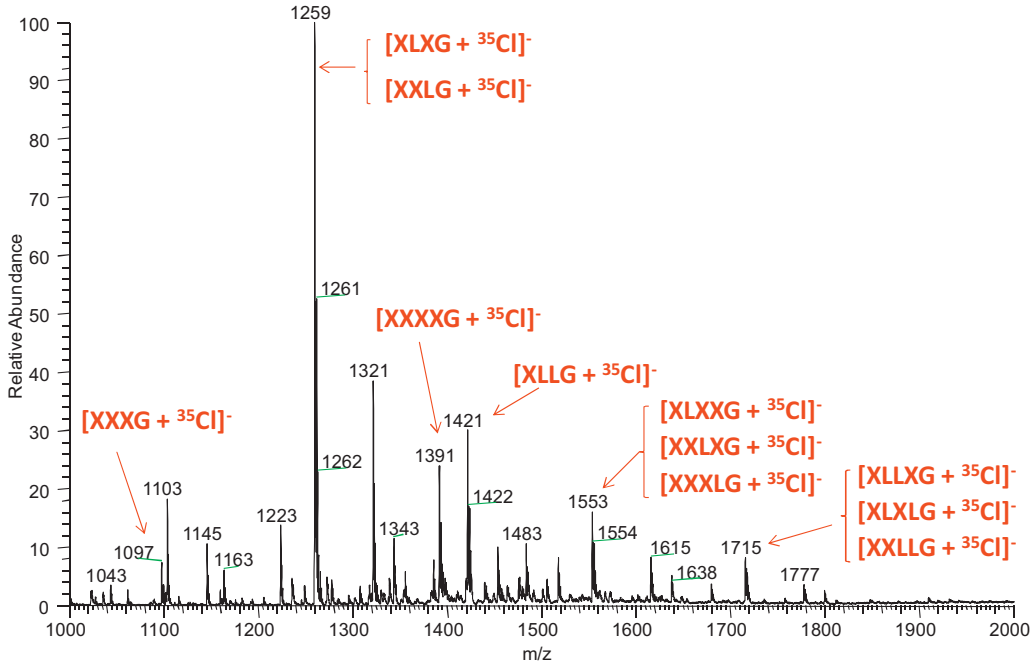

Fig. 8. Mass spectrum obtained for xyloglucan oligomers derived from *Hymenaea courbaril* by chloride anion attachment ESI/MS.

subjected to CAD, as discussed above. This ion is produced from the deprotonated XXXLG oligomer (Supplemental information, Figure 4). Hence, it is possible to verify the presence of the three isomers that were observed in the HPAEC profile (Fig. 2).

Finally, CAD of the last anion examined for *Hymenaea*, the chloride anion adduct of XLLXG (*m*/*z* 1715), generates the fragment anions of *m*/*z* 1679, 1619, 1601, 1517, 1439 and 1223, among others. The deprotonated XLLXG (*m*/*z* 1679) was isolated and subjected to CAD (MS^3), which generated the fragment anions of *m*/*z* 1619, 1601, 1517, 1439, 1223 and less of the fragment anion of *m*/*z* 767. The fragment anions of *m*/*z* 1619 and 1601 are formed via loss of $C_2H_4O_2$ and $C_2H_4O_2 + H_2O$, respectively. The anion of *m*/*z* 1517 is formed via the loss of a glucose residue to give deprotonated XLLX, and the anion of *m*/*z* 1439 is formed via the loss of $C_2H_4O_2$ and H_2O. The fragment anion of *m*/*z* 1223, which represents deprotonated XLL, is formed via loss of a xylose–glucose residue (X, MW of 294 Da). The anion of *m*/*z* 1223 was isolated for CAD (MS^4) and this generated the fragment anions of *m*/*z* 1163, 1145, 767, 707 and 689, among others. The most abundant one is the anion of *m*/*z* 767, which is formed via the loss of a galactose–xylose–glucose residue (L, MW of 456 Da) to give the characteristic deprotonated XL (*m*/*z* 767) (Supplemental information, Figure 5). These results indicate that the fragmentation of deprotonated XyGs upon CAD occurs in a stepwise manner starting from the reducing end, which facilitates the sequencing of XyGs.

4. Conclusions

The sodium cation adducts formed in an ESI source for XyGs in this study proved to be useful in the MW determination of the XyG oligomers in mixtures. This is a good first step toward the characterization of these oligomers in mixtures since the impurities in the XyG solutions (as prepared here) are less likely to be ionized in positive ion than in negative ion mode. However, structural information was difficult to obtain by examining dissociation reactions of the sodium adducts of XyGs. The combination of ESI with chloride anion dopant and multiple-stage tandem mass spectrometry has proven to be an excellent method for the structural characterization of enzyme digests containing xyloglucan oligomers. Only xyloglucans were found to form chloride anion adducts. The chloride anion adducts of the xyloglucans fragment predominantly by loss of HCl (MS^2 experiment). This specific loss can be used to verify that the fragmenting ion is a chloride anion adduct, and hence confirm the molecular weight (MW) of the analyte.

The fragmentation patterns of the deprotonated molecules generated upon HCl loss from the chloride anion adducts of xyloglucans can be used to differentiate between isomeric oligomers since it allows sequencing of the xyloglucans. The multiple-stage tandem mass spectra obtained this way for enzyme digests of *Arabidopsis Columbia-0* and *H. courbaril* reveal the same oligomer profile observed for HPAEC, which suggests that this mass spectrometric method can be used to quantify xyloglucans.

Acknowledgements

This work was supported as part of the Center for Direct Catalytic Conversion of Biomass to Biofuels (C3Bio), an Energy Frontier Research Center funded by the U.S. Department of Energy, Office of Science, Office of Basic Energy Sciences under Award Number DE-SC0000997. Wolf-Dieter Reiter, University of Connecticut and Dr. Marcos Buckeridge, University of São Paulo, Brasil, are thanked for providing Arabidopsis seeds and Hymenaea xyloglucans, respectively.

Appendix A. Supplementary data

Supplementary data associated with this article can be found, in the online version, at http://dx.doi.org/10.1016/j.carbpol.2013.06.070.

References

Buckeridge, M. S. (2010). Seed cell wall storage polysaccharides: Models to understand cell wall biosynthesis and degradation. *Plant Physiology*, *154*, 1017–1023.
Cai, Y., & Cole, R. B. (2002). Stabilization of anionic adducts in negative ion electrospray mass spectrometry. *Analytical Chemistry*, *74*, 985–991.

Cai, Y., Jiang, Y., & Cole, R. B. (2003). Anionic adducts of oligosaccharides by matrix-assisted laser desorption/ionization time of-flight mass spectrometry. *Analytical Chemistry*, *75*, 1638–1644.

Carpita, N. C., & Gibeaut, D. M. (1993). Structural models of primary cell walls in flowering plants: Consistency of molecular structure with the physical properties of the walls during growth. *Plant Journal*, *3*, 1–30.

Fry, S. C. (1993). An unambiguous nomenclature for xyloglucan-derived oligosaccharides. *Physiologia Plantarum*, *89*, 1–3.

Hoffman, M., Jia, Z., Peña, M. J., Cash, M., Harper, A. A. R. B., Darvill, A., et al. (2005). Structural analysis of xyloglucans in the primary cell walls of plants in the subclass Asteridae. *Carbohydrate Research*, *340*, 1826–1840.

Jiang, Y., & Cole, R. B. (2005). Oligosaccharide analysis using anion attachment in negative mode electrospray mass spectrometry. *Journal of the American Society for Mass Spectrometry*, *16*, 60–70.

Madson, M., Dunand, C., Verma, R., Vanzin, G. F., Caplan, J., Li, X., et al. (2003). Xyloglucan galactosyltransferase, a plant enzyme in cell wall biogenesis homologous to animal exostosins. *Plant Cell*, *15*, 1662–1670.

Pfenninger, A., Karas, M., Finke, B., & Stahl, B. (2002). Structural analysis of underivatized neutral human milk oligosaccharides in the negative ion mode by nano-electrospray MS^n. Part 1. Methodology. *Journal of the American Society for Mass Spectrometry*, *13*, 1331–1340.

Reiter, W.-D., Chapple, C., & Somerville, C. R. (1997). Mutants of *Arabidopsis thaliana* with altered cell wall polysaccharide composition. *Plant Journal*, *12*, 335–345.

Sims, I. M., Munro, S. L. A., Currie, G., Craik, D., & Bacic, A. (1996). Structural characterisation of xyloglucan secreted by suspension cultured cells of *Nicotiana plumbaginifolia*. *Carbohydrate Research*, *293*, 147–172.

Tiné, M. A. S., Clovis, C. O., de Lima, D. U., Carpita, N. C., & Buckeridge, M. S. (2006). Fine structure of a mixed-oligomer storage xyloglucan from seeds of *Hymenaea courbaril*. *Carbohydrate Polymers*, *66*, 444–454.

Vanzin, G. F., Madson, M., Carpita, N. C., Raikhel, N. V., Keegstra, K., & Reiter, W.-D. (2002). The *mur2* mutant of *Arabidopsis thaliana* lacks fucosylated xyloglucan because of a lesion in fucosyltransferase AtFUT1. *Proceedings of the National Academy of Sciences of the United States of America*, *99*, 3340–3345.

Vinueza, N. R., Gallardo, V. A., Carpita, N. C., & Kenttämaa, H. I. (2013). Analysis of carbohydrates by atmospheric pressure chloride anion attachment tandem mass spectrometry. *Fuel*, *105*, 235–246.

Zhu, J. H., & Cole, R. B. (2000). Formation and decompositions of chloride adduct ions, M + Cl (−), in negative ion electrospray ionization mass spectrometry. *Journal of the American Society for Mass Spectrometry*, *11*, 932–941.

Zhu, J., & Cole, R. B. (2001). Ranking of gas-phase acidities and chloride affinities of monosaccharides and linkage specificity in collision-induced decompositions of negative ion electrospray-generated chloride adducts of oligosaccharides. *Journal of the American Society for Mass Spectrometry*, *12*, 1193–1204.